Technische Universität München

Fakultät für Medizin

Klinik und Poliklinik Innere Medizin 1

Klinikum rechts der Isar

(Direktor: Prof. Dr. Karl-Ludwig Laugwitz)

Hybrid PET/MR Imaging for the Prediction of Left Ventricular Recovery after Percutaneous Revascularization of Chronic Total Occluded Coronaries

Teresa Vitadello

Vollständiger Abdruck der von der Fakultät für Medizin der Technischen Universität München zur Erlangung des akademischen Grades eines

Doktors der Medizin

genehmigten Dissertation.

Vorsitzender: Prof. Dr. Wolfgang Weber
Prüfer der Dissertation:
1. apl. Prof. Dr. Tareq Ibrahim
2. Priv.-Doz. Dr. Stephan Nekolla
Die Dissertation wurde am 28.04.2020 bei der Technischen Universität München eingereicht und durch die Fakultät für Medizin am 06.10.2020 angenommen.

Table of contents

List of tables

List of Figures

List of Abbreviations

AHA	American Heart Association
AUC	Area Under the Curve
CAD	Coronary Artery Disease
CTO	Chronic Total Occlusion
FDG	Fluorodeoxyglucose
EF	Ejection Fraction
EDV	Enddiastolic Volume
ESC	European Society of Cardiology
ESV	Endsystolic Volume
FFR	Fractional Flow Reserve
Gd-DTPA	Gadopentetat-Dimeglumin
ICD	Implantable Cardioverter Defibrillator
LAD	Left Anterior Descending
LCx	Left Circumflex
LV	Left Ventricular
LGE	Late Gadolinium Enhancement
MACE	Major Adverse Cardiovascular Events
MRI	Magnetic Resonance Imaging
PET/MR	Positron Emission Tomography/Magnetic Resonance
PCI	Percutaneous Coronary Intervention
PSIR	Phase-Sensitive, Inversion-Recovery prepared T1-weighted gradient-echo pulse Sequences
ROC	Receiver Operating Curve
SE	Standard Error
TIMI	Thrombolysis in Myocardial Infarction
WMA	Wall motion abnormality

1. Abstract

1.1. Background

Percutaneous coronary intervention (PCI) of chronic total occlusion (CTO) represents one of the major challenges in interventional cardiology. Physicians are still reluctant in referring for PCI, assuming non-viability of the myocardium subtended by the CTO. Data are controversial in assessing the improvement of left ventricular (LV) wall motion after revascularization and the prognostic value of viability testing to guide patient selection.

1.2 Objective

This study sought to determine the value of viability testing with hybrid fluorodeoxyglucose positron emission tomography/magnetic resonance (FDG PET/MR) imaging in predicting left ventricular (LV) wall motion recovery after revascularization of coronary chronic total occlusion (CTO) in comparison to PET or MRI alone.

1.3 Methods

49 consecutive symptomatic patients with CTO and evidence of wall motion abnormality in the corresponding CTO-territory were enrolled. All patients underwent hybrid FDG PET/MR imaging as semi-quantitative assessment of myocardial viability (i.e. maintained glucose metabolism) in PET and late gadolinium enhancement (LGE) transmurality in magnetic resonance imaging (MRI) – prior to PCI of the CTO. Follow-up MRI was performed in 23 patients 3-6 months after successful revascularization to evaluate wall motion recovery.

1.4 Results

We assessed viability in 124 myocardial segments subtended by a CTO in 23 patients with successful PCI, who underwent serial imaging. Segments with wall motion abnormality at baseline (n=80) were analyzed. Most of these segments (n=54, 68%) were concordantly assessed viable by PET and MRI, conversely only 2 (2%) segments were assessed non-viable by both imaging modalities. However, 30% showed a discordant viability pattern, either PET non-viable/ MRI viable (3 segments, 4%) or PET viable/ MRI non-viable (21 segments, 26%) and the latter revealed a significant wall motion improvement at follow-up (p=0.033). Combined imaging by FDG PET/MR showed a fair accuracy in predicting myocardial recovery after CTO revascularization (PET/MR area under ROC curve (AUC) 0.72, SE 0.07, p=0.002), which was superior to MRI-LGE (AUC=0.66) and FDG-PET (AUC=0.58) alone.

1.5 Conclusion

Hybrid PET/MR imaging prior to CTO revascularization predicts more accurately the recovery of dysfunctional myocardium than PET or MRI alone. The complimentary information derived from both modalities may particularly help to identify small amounts of viable epicardial myocardium within large scars, which can improve contractility after CTO-revascularization.

2. Zusammenfassung

2.1. Hintergrund

Bei Patienten mit chronischen totalen Verschlüssen der Koronararterien ist die Datenlage aktuell nicht eindeutig, ob eine perkutane Revaskularisierung zu einer Verbesserung der linksventrikulären Pumpfunktion und somit auch zu einer verbesserten Prognose führen kann.

2.2 Ziel

Ziel dieser prospektiven Studie war es zu untersuchen, ob eine Vitalitätsevaluation mittels kombinierter Fluordesoxyglukose Positronen-Emissions-Tomografie/ Magnetresonanztomografie (FDG PET/MRT) eine genauere Stratifizierung hinsichtlich einer Verbesserung der linksventrikulären Funktion im Vergleich zu FDG PET oder MRT alleine ermöglicht.

2.3 Methodik

49 Patienten mit einer relevanten CTO und einer regionalen Wandbewegungsstörung im korrespondierenden Versorgungsgebiet wurden prospektiv eingeschlossen und mittels FDG PET/MRT untersucht. Nach Durchführung des FDG PET/MRTs und Evaluation der Vitalität (Glucosemetabolismus im PET bzw. Transmuralität des „late gadolinium enhancements“ (LGE) im MRT) der betroffenen Segmente im AHA 17-Segment-Modell wurde eine perkutane Revaskularisierung durchgeführt. Zur Beurteilung der linksventrikulären myokardialen Funktionsverbesserung wurde eine MRT nach ca. 3-6 Monaten durchgeführt.

2.4 Ergebnisse

Von 23 erfolgreich revaskularisierten Patienten mit MRT-Follow-up wurden die 80 betroffenen Segmente im Versorgungsgebiet der CTO analysiert, wobei 93% (75/80) PET-vital waren, während im MRT nur 71% (57/80) eine Vitalität aufwiesen. 68% (54/80) der Segmente waren konkordant PET/MRT vital und 2% (2/80) konkordant PET/MRT avital. 30% der Segmente wiesen ein diskrepantes Ergebnis auf: 4% (3/80) als PET avital/MRT vital bzw. 26% (21/80) der Segmente als PET vital/MRT avital gewertet wurden. Die letzten zeigten eine signifikante funktionelle Verbesserung bei der Follow-Up Untersuchung ($p=0.033$). Die Kombination von FDG PET/MRT erlaubt eine genauere Vorhersage der Verbesserung der regionalen Wandbewegung nach Revaskularisation (PET/MRT Fläche unter der ROC Kurve (AUC) 0.72, SE 0.07, $p=0.002$), im Vergleich zu MRT-LGE (AUC=0.66) oder FDG-PET (AUC=0.58) allein.

2.5 Schlussfolgerungen

Die kombinierte FDG PET/MRT Bildgebung erlaubt eine bessere Stratifizierung hinsichtlich einer LV-Funktionsverbesserung nach Revaskularisation im Vergleich zu PET oder MRT allein. Die durch die beiden Modalitäten zusätzlich erbrachten Informationen können dabei helfen kleine Areale von vitalem Myokard zu identifizieren, die nach einer Revaskularisation die Kontraktilität steigern können.

3. Introduction

3.1 Epidemiology of cardiovascular disease and coronary chronic total occlusions

Cardiovascular disease represents one of the major cause of death and disability in developed countries, accounting for over 3.8 million deaths each year, or 45% of all deaths across European Society of Cardiology (ESC) member countries (Timmis et al. 2018). In patients with coronary artery disease (CAD), atherosclerosis leads to the narrowing of coronary arteries resulting in hemodynamically significant coronary lesions that induce myocardial ischemia. Among those patients undergoing coronary angiography, the incidence of at least one coronary chronic total occlusion (CTO) has been reported in literature to be up to 30 to 50% (Koelbl et al., 2018). A CTO is defined on a native coronary artery presenting an atherosclerotic complete vessel narrowing with interruption of antegrade blood flow (Thrombolysis in Myocardial Infarction [TIMI] grade 0 flow) and an estimated occlusion duration of ≥ 3 months (Koelbl et al., 2018). The overall prevalence of chronic total occlusions in the general asymptomatic population is unknown.

A CTO could evolve after an acute myocardial infarction - even in 30 to 45% of patients before PCI was routinely used in such a clinical setting. Thanks to PCI, rates have dropped, but a CTO might develop after a failed intervention or subsequent vessel reocclusion in 5–10% of patients who underwent myocardial infarction. Moreover, approximately 40% of patients with a CTO had a history of previous myocardial infarction, which is twice as high as in patients without a CTO (Hoebers et al., 2014).

3.2 Percutaneous coronary intervention of coronary chronic total occlusions

Percutaneous coronary intervention (PCI) of CTOs represents one of the major challenges in interventional cardiology (Suero et al., 2001), and has historically been performed in only 10% to 15% of all affected patients (Koelbl et al., 2018). The discrepancy between the prevalence of CTOs and the lower rate of invasive revascularization highlights the technical complexity and perceived risk of complications compared with medical therapy, but also the clinical uncertainties regarding patient selection before PCI (Hoebers et al., 2014). Nevertheless, due to the recent development of the interventional retrograde approach and the dual arterial access, the improvement in guidewire technology, and implementation of dissection and re-entry strategies, the success rate has increased to 80-90%, when revascularization is performed by experienced operators. Moreover, the rate of periprocedural major adverse cardiovascular events (MACE) does not appear to be higher than with non-CTO lesions (Suero et al., 2001). Several other studies suggest that successful CTO revascularization is associated with symptom relief and improvement in quality of life, a higher electrical myocardial stability, a reduced need for bypass surgery, an enhanced tolerance of future coronary events, the recovery of left ventricular function and improved survival in comparison to failed PCI (Galassi et al. 2015, Stuijfzand et al., 2017, Hoebers et al., 2014), other randomised controlled studies are still ongoing in order to validate those findings. Recently, the prospective randomized EUROCTO (Randomized Multicentre Trial to Compare Revascularization With Optimal Medical Therapy for the Treatment of Chronic Total Occlusions) trial showed symptomatic improvement by PCI of CTO in comparison to optimal medical therapy alone and comparable rate of MACE between the two groups.

The “Drug-Eluting Stent Implantation Versus Optimal Medical Treatment in Patients With Chronic Total Occlusion” (“DECISION-CTO”) trial (ClinicalTrials.gov identifier NCT 01078051) showed that the recanalization of a CTO was non-inferior but also not superior

to optimal medical therapy, when compared towards a combined primary endpoint (mortality, myocardial infarction, stroke and any revascularization at 3 years), due primarily to low enrollment (Koelbl et al., 2018). ACCF/AHA/SCAI PCI Guideline 2011 assigned a Class IIa indication with level of evidence B to revascularization of a CTO and suggested PCI after an individualized risk-benefit assessment encompassing clinical, angiographic and technical considerations (Levine et al., 2011). Moreover, 2018 ESC/EACTS Guidelines suggest the sought of objective evidence of viability before revascularization, in the presence of regional wall motion abnormalities in the territory of the CTO.

3.3 Myocardial ischemia and viability in the presence of a CTO

Occurring as a chronic process, CTOs allow for development of collateral arteries from other coronary beds. In the presence of a CTO, collateral flow is assumed to be sufficient in preventing ischemia or that the myocardium subtended by the occluded artery is likely to be non-viable (Stuijfzand et al., 2017). Though collaterals to CTO are often essential to keep the myocardial viability, they are not able to provide sufficient blood flow reserve in case of increased myocardial requirements (Koelbl et al., 2018). This hypothesis was confirmed in a study through the measurement of Fractional flow reserve (FFR), an invasive diagnostic tool used during coronary angiography to assess the hemodynamic relevance of a coronary lesion. All CTO patients showed an ischemic FFR, even in the presence of severe regional wall motion dysfunction or well−developed collaterals (Sachdeva et al., 2014). After a successful CTO revascularization, Sachdeva et al. (2014) showed an improvement of myocardial hemodynamics through invasive flow measurements comparable to a non-CTO PCI. Therefore, in symptomatic patients CTO subtend ischemic regions, even in the presence of an excellent collateral development and a successful revascular-

ization reduces the burden of ischemia. Moreover, Stuijfzand et al. confirmed through PET perfusion studies the hypothesis of a significant perfusion impairment in the vast majority of CTO patients with a preserved LVEF, even in the presence of angiographically well-developed collateral arteries. The collateral function during increased blood flow demand in viable myocardium was predominantly insufficient, indicating the need of revascularization. Moreover, since the angiographic assessment of collaterals cannot accurately predict myocardial viability, and has lower sensitivity in prediction of functional improvement in CTO territories after revascularization, the evaluation of myocardial viability with non-invasive imaging modalities is necessary (Wang et al., 2018). It has been recently studied that in patients with CTOs, the extent of myocardial hibernation and scar does not correlate to the angiographic status of the collateral flow (Wang et al. 2018).

Myocardium supplied by a CTO may have various pathophysiological features, ranging from normal perfusion to stress-induced ischemia, stunning, hibernation, and eventually necrosis. The assessment of myocardial function, viability and ischemia, by means of a reliable diagnostic test, helps in predicting the benefits of the successful revascularization of a CTO (Bucciarelli-Ducci et al, 2016), such as functional improvement. Therefore, it improves patient selection in the clinical routine through an additional risk assessment (Stuifwand et al., 2017). Many non-invasive imaging modalities such as positron emission tomography (PET), and cardiac magnetic resonance (MR) have been developed for the identification and assessment of myocardial viability. Both PET and MR imaging have been available in the clinical practice for more than 20 years and have developed as highly valuable diagnostic tools. PET investigation is considered the most reliable noninvasive procedure in the assessment of myocardial metabolism and perfusion in the CAD evaluation (Nekolla et al., 2009). Meanwhile, contrast-enhanced MR imaging of the heart has been increasingly used to assess myocardial viability. Given its high spatial resolution, it

allows the acquisition of both cardiac function and transmural definition of myocardial scarring, the latter using mainly Late Gadolinium Enhancement (LGE) methods.

3.4. Positron emission tomography

PET is an imaging technique, which employs tracers labeled with a positron-emitting isotope in order to produce images of in vivo metabolism of an organ, more than anatomy. Depending on the radiotracer, PET imaging allows non invasive evaluation of of myocardial blood flow, function and metabolism, measuring radionuclide distribution with an external detector system (Dilsizian et al., 2009). During PET acquisition, two opposite gamma photons of 511 keV – almost exactly 180° apart – are generated from the annihilation event caused by a positron interacting with an electron (Figure 1). Detectors are placed as rings around the patient: sensing almost simultaneously the two gamma photons from the annihilation event, the annihilation is presumed occurring along the line between the two opposite detectors (Anagnostopoulos et al., 2013, Cassen 1964). Combining these signal acquisitions, cross-sectional slice images are developed from the spatial (and optionally temporal distribution) of the radiotracer.

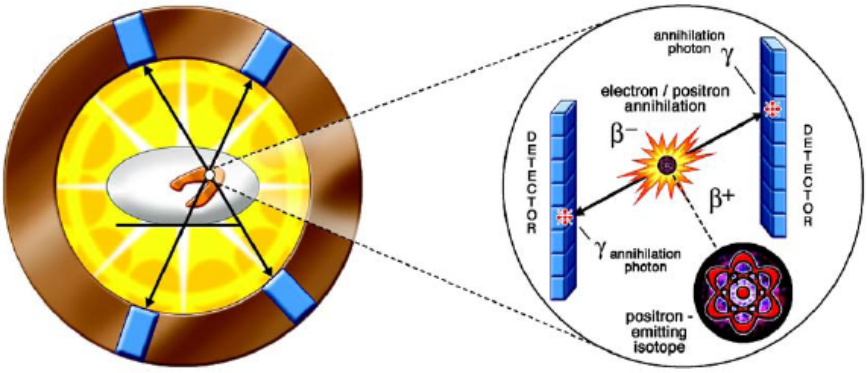

Figure 1. Radiopharmaceuticals such as ^{13}N emit positrons (β^+), which collide with electrons (e^-), after travelling through matter and losing their energy. β^+ and e^- are antiparticles: at collision, a reaction called "annihilation" occurs, generating two photons which are emitted at a 180° angle. The photons are detected simultaneously from the detector ring. Adapted from "Cardiac PET imaging for the detection and monitoring of coronary artery disease and microvascular health" by Schindler et al., 2010.

3.5 FDG PET metabolic imaging

The most relevant tracer in clinical cardiac PET myocardial viability imaging is ^{18}[F]-Fluorodeoxyglucose (FDG), which is a radiolabeled glucose analog and is used to image myocardial glucose utilization in vivo (Gambhir et al.,1989; Schwaiger et al., 1987). ^{18}[F]-FDG is widely available as it is also extensively used in oncologic diagnostics. FDG-PET represents the clinical "gold standard" in the investigation of myocardial viability, is the most commonly used PET tracer to image the hibernating myocardium. Viable myocardium is typically identified by the presence of >50% relative glucose uptake in the myocardium (Rischpler et al., 2015; Allmann et at., 2013). In physiological conditions nonischemic myocardial metabolism is based on the utilization of fatty acids in fasting state and glucose in

the post- prandial state, whereas ischemia promotes the switch to glycolysis. Therefore, ischemic and dysfunctional myocardium presents a maintained or even increased glucose uptake. For the evaluation of myocardial viability with FDG, the substrate and hormonal levels in the blood need to favor utilization of glucose over fatty acids by the myocardium. The physical half-life of ^{18}[F] is 110 min and ^{18}[F]-FDG uptake into the myocardium is dependent on the insulin-sensitive glucose transporters (Sarikaya et al., 2015). Through the euglycemic hyperinsulinemic clamp - a rigorous but rather time-consuming procedure with simultaneous administration of glucose and insulin i.v. - it is possible to titrate precisely the metabolic substrates and insulin levels, which results in excellent image quality in most patients (Dilsizian et al., 2009). Once taken up by the myocardial cells, ^{18}[F]-FDG is phosphorylated into ^{18}[F]-FDG-6-phosphate and becomes trapped in the myocardial cells, as it minimally undergoes subsequent metabolism and its dephosphorylation rate is slow (Sarikaya et al., 2015).

The sensitivity of ^{18}[F]-FDG PET imaging to detect viable (or hibernating) myocardium is high: the prediction of improvement in regional function after revascularization by dobutamine echocardiography, Tl-201 and Tc-99m scintigraphy, PET, and MR was compared in a pooled analysis of viability studies from 1980 through to January 2007: the weighted mean sensitivity, specificity, positive predictive value, and NPV of ^{18}[F]-FDG PET were 92, 63, 74, and 87%, respectively, (Schinkel et al, 2007). ^{18}[F]-FDG PET showed the highest sensitivity and dobutamine echocardiography the highest specificity compared with other methods for the prediction of recovery of regional function after revascularization (Schinkel et al, 2007).

3.6 Magnetic Resonance imaging

MR is an imaging technique that generates and acquires images with high temporal and spatial resolution and an excellent rendering of the soft tissues, through the exposure to magnetic fields and electromagnetic waves in the radio frequency domain (Santarelli MF et al., 2005). Different biological properties and characteristics of tissues, such as proton density or spin relaxation times T_1 (longitudinal relaxation time) and T_2 (transversal relaxation time), are assessed from the MR signal released from the sample. The acquisition of these particular parameters allows to discriminate different tissue types or pathologic alterations in biological tissue. In comparison to the majority of the imaging techniques, MR imaging is performed using non-ionizing radiation: therefore, when used within the approved limits, it is considered non-hazardous. However, contraindications to MR include metallic implantable devices, such as pacemaker and Implantable Cardioverter Defibrillator (ICD), and this is often the case in patients with severely reduced ventricular pump function.

3.7 Cardiac magnetic resonance and viability evaluation

Currently, cardiac MR imaging is considered as a standard tool for morphologic characterization of the myocardium and has been established as the gold standard for assessment of ventricular function, given its high spatial resolution (Krumm et al. 2018). Several cardiac MR techniques have been proposed for the assessment of myocardial viability. These techniques include resting cardiac MR (end diastolic wall thickness), dobutamine CMR (contractile reserve), and contrast enhanced CMR (scar tissue). Contrast enhanced MR viability imaging has been established in as a reliable modality, in which the assessment of Late Gadolinium Enhancement (LGE) allows the definition of myocardial scar in its extent

of transmurality, distinguishing transmural from subendocardial myocardial injuries, which represents also prognostic relevance (Kwong et al. 2006). LGE is performed 5–20 min after the administration of contrast media Gadopentetat-Dimeglumin (Gd-DTPA) using inversion-recovery prepared T1-weighted gradient-echo pulse sequences (PSIR) to suppress the signal from remote myocardium and allows the identification of scarred myocardium and is defined as regions of increased image intensity on T1 weighted images (Kaandorp et al, 2005). Due to its higher spatial resolution, LGE imaging has shown advantages in detecting small sub-endocardial scars as compared with PET (Krumm et al., 2018) and can predict improvement of depressed myocardial function after revascularization (Kirschbaum et al., 2012). The enhancement is due to changes in the extracellular matrix between collagen fibres, which is in larger amount in scar tissue as compared to the densely packed viable myocardium, and the contrast agent has an increased volume of distribution in the interstitial volume (Kaandorp et al., 2005). LGE is validated and now widely performed to a high standard (Klein et al., 2002) and is used as a surrogate endpoint in therapeutic studies, such as adjuvant treatment in acute infarction (Captur et al 2016).

3.8 Hybrid PET/MR Imaging

Fully integrated PET/MR systems allow the simultaneous acquisition of both modalities and offer the unique opportunity to merge PET and MRI features both spatially and temporally, combining high resolution anatomy and high sensitivity for the detection of molecular targets, as well as highly time-resolved functional parameters such as wall motion. The Siemens Biograph mMR was the world's first system able to combine MRI and PET imaging simultaneously in one scanner. Moreover, the simultaneous image acquisition reduces

the examination time with optimized co-registration at similar time points (Krumm et al., 2018).

In the past, both imaging modalities approaches have been shown to produce valuable data for the prediction of functional outcome of the myocardium after revascularization (Shah et al. 2013), but synergistic effects are still unknown. Moreover, in patients with CTO, studies investigating these techniques with respect to clinical outcome are scarce. Therefore, the aim of this thesis was to determine whether hybrid FDG-PET/MR imaging allows for more accurate prediction of regional left ventricular recovery after successful percutaneous revascularization of a CTO in symptomatic patients in comparison to PET or MR alone.

4. Methods

4.1 Study design

Between February 2016 to January 2018 we prospectively enrolled 49 consecutive patients with symptomatic CAD (angina or angina equivalent) due to the presence of a CTO of a relevant coronary artery (segment 1, 2, 6, 7, 11 or 13, diameter >2,5 mm) and evidence of corresponding wall motion abnormality either assessed by echocardiography or angiography. Recruitment was performed at 3 different institutions: Klinikum Rechts der Isar, Deutsches Herzzentrum and Osypka Herzzentrum in Munich. All patients underwent hybrid FDG PET/MR imaging before undergoing CTO revascularization. Exclusion criteria included contraindications for PET/MRI (pregnancy, hemodynamic instability, estimated glomerular filtration <30ml/min, allergy to contrast agent, claustrophobia, presence of pacemakers, ICDs, or any other ferromagnetic material in the body). To evaluate the impact of the procedure on the left ventricular function, a follow-up MRI was scheduled within 6 months after successful CTO revascularization and was obtained in n=23 patients. Follow-up imaging was not performed in 26 patients due to different reasons including unsuccessful revascularization of the CTO (n=15), not performed revascularization of the CTO (n=6), meanwhile implantation of MRI-incompatible pacemaker/ICD (n=1) or loss to follow-up (n=3). Furthermore, one patient had to be removed from the final analysis because of poor image quality of the PET scan.

The study was approved by the local ethics committee (vote of approval 169/16 S) and was performed in agreement with the ethical standards according to the Declaration of Helsinki. For all patients written informed consent was obtained prior to imaging.

4.2 Imaging protocol

Imaging was performed in all patients using a hybrid PET/MRI system (Biograph mMR, Siemens Medical Solutions, Erlangen, Germany), which acquires simultaneously PET and MRI data (Figure 2). The MRI component consists of a 3 Tesla MRI scanner, while the PET component is built of LSO crystals equipped with avalanche photodiodes (Torigian et al. 2013). The performance of the PET/MRI system has been previously evaluated in different studies (Delso et al. 2011).

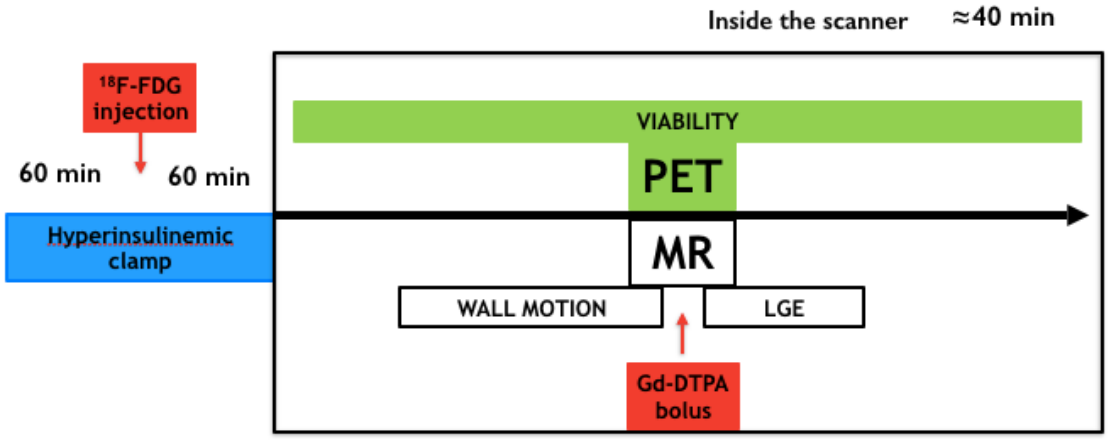

Figure 2. PET/MRI viability protocol: the hyperinsulinemic clamp for approximately 60 minutes precedes the FDG injection. After 60 minutes begins the scan with the simultaneous acquisition of PET and MRI sequences. After the acquisition of cine sequences, Gd-DTPA is injected.

4.3. PET imaging

In order to reach the optimal uptake of glucose within the myocardium, the hyperinsulinaemic-euglycaemic clamp technique was applied to standardize the metabolic environment in all patients (DeFronzo et al., 1979). The insulin pump was prepared with 0,06 U/kg/KG/h insulin (or 0,1 U/kgKG/h in diabetic patients) diluted in 50 ml 0,9% NaCl solution. Meanwhile plasma glucose was determined every 10 minutes. After the stabilization of the plasma glucose level for approx. 60 minutes through the clamp technique, 240-370 MBq FDG (4MBq per kg body weight) was administered intravenously. Approximately 60 minutes after the intravenous injection of FDG, a list-mode PET scan in 3D mode was started. The acquisition was performed applying ECG gating. Emission data were corrected for dead time, randoms, scatter, and attenuation. Images were reconstructed using a 3D attenuation-weighted ordered subsets expectation maximization iterative reconstruction algorithm (AW-OSEM 3D) with three iterations and 21 subsets, Gaussian smoothing at 4 mm full width at half maximum, a matrix size of 344 x 344, and a zoom of 1. 2-point Dixon MRI sequences were used in the attenuation correction of PET data, as previously described (Martinez-Moller et al, 2009). Since parts of the body may be truncated in the attenuation map, because of the relatively small field of view of the MRI, the recovery of the missing part of the attenuation map was assessed from PET emission data, using the so-called maximum likelihood reconstruction of attenuation and activity (MLAA) technique, as previously described (Nuyts et al., 2013). PET images are acquired simultaneously to MR images.

4.4 MR imaging

After positioning the patient, overview images (scout) of the heart in the 3 standard sectional planes (axial, coronal, sagittal) were acquired. Firstly, MR sequences without contrast agents were planned on the basis of these sectional planes: - ECG triggered sequences for functional diagnostics (BFFE, CINE-sequences): primary visualisation of the left ventricle in the 4-chamber view, 2-chamber view, and short axis. Thereafter, 0.2 mmol/kg Gd-DTPA (Magnograf; Marotrast GmbH, Jena, Germany) was administered intravenously after a waiting time of at least 10 minutes LGE data were acquired, using an inversion recovery-prepared T1-weighted gradient-echo pulse sequences with phase-sensitive reconstruction (PSIR). For left ventricular wall motion analyses, steady-state free precession cine sequences were acquired. ECG triggering was applied for the acquisition of these sequences, and all images — including long-axis (two-chamber view and four-chamber view) and short-axis views of the entire left ventricle—were obtained during breath hold. For the entire scan, phased-array body surface coils were used.

4.5 Image analysis

All modalities were analyzed using a dedicated software package (Munich Heart), which allowed the depiction of quantitative measures in polar maps, on which an established 17-segment model according to the American Heart Association (AHA) (Cerqueira et al. 2002) were applied (Nekolla et al.,1998).

For PET analysis, the maximal uptake of FDG within the left ventricle was set as reference and the segments were defined viable if their FDG uptake was at least 50% of the refer-

ence area (Baer et al., 1996). In case of an FDG uptake below this threshold, the respective segment was defined as ‘FDG non-viable’ (Rischpler et al, 2015).

MRI analysis were performed independently by two experienced observers, who were blinded for the angiographic data. Global LV function parameters, such as LV mass, end systolic volume (ESV), enddiastolic volume (EDV), and ejection fraction (EF) were analyzed by manual outlining of the left ventricular contours on short-axis cine images using the MunichHeart/MR software (Figure 3 and 4). Similarly, the amount of LGE was manually traced on each short-axis slice and calculated as percentage of the left ventricle (Rischpler et al, 2015). Regional transmural extent of LGE was determined for each LV segment according to a 5-point score: 0=no, 1≤25%, 2≤50%, 3≤75%, 4>75-100% LGE. If the transmural extent of LGE was ≤50% (Score 0-2) of the myocardial thickness, the segment was defined ‘MRI viable’, and for any extent >50% (Score 3,4) as ‘MRI non-viable’, respectively. Moreover, regional wall motion was semiquantitatively assessed at baseline and follow-up in each segment using a 5-point scale (0 = normal wall motion, 1 = mild to moderate hypokinesia, 2 = severe hypokinesia, 3 = akinesia, and 4 = dyskinesia) defining the degree of wall motion impairment in each of the 17 myocardial segments at baseline and follow-up. A decrease of the wall motion abnormality score of at least 1 point was defined as contractility improvement.

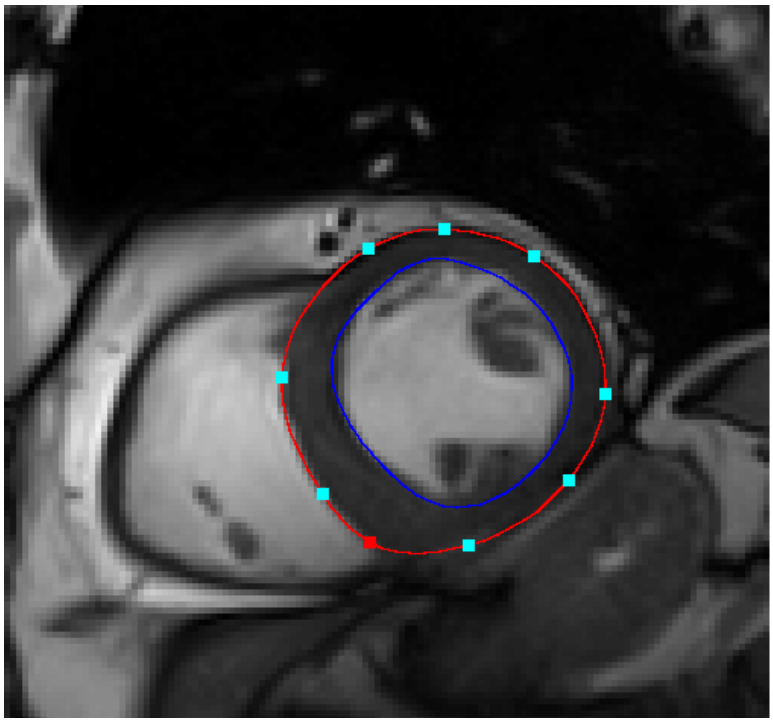

Figure 3. Example of myocardial volumes and ejection fraction quantification through MR postprocessing. In short axis slices myocardial contours are defined in red (epicardial) and blue (endocardial). Imaging post processing has been done through Munich Heart/ MR Myocardial Wall Tool 1.8.5.0.

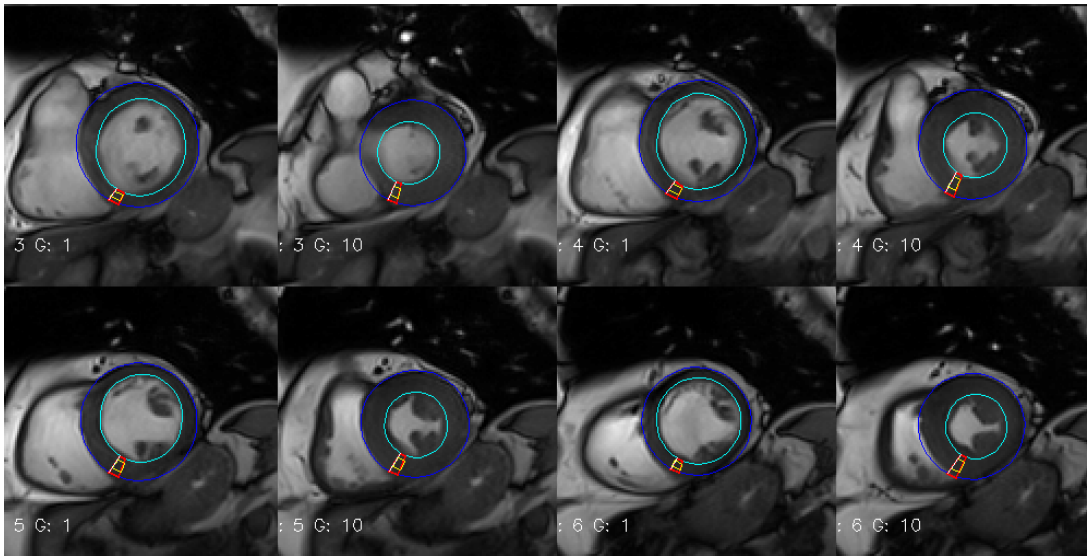

Figure 4. End diastolic (1) and end systolic (10) gates of MR short axis slice images (3,4,5,6). Epicardial and endocardial contours are drawn in blue and light blue, respectively. Munich Heart/ MR Myocardial Wall Tool 1.8.5.0 Beta.

4.6 Statistics

The distribution of quantitative data is presented by mean ± standard deviation (SD) or median (interquartile range, IQR), as appropriate. Comparisons of baseline and follow-up measurements were performed by t-tests for paired samples. The distribution of ordinal variables was compared between cohorts using the Mann Whitney-U test. Quantitative data is presented by absolute and relative frequencies. Intermethod agreement was calculated by means of Cohen's Kappa.

Changes of regional wall motion and of measurements of LGE between baseline and follow-up were tested by the Wilcoxon signed rank test due to deviations from the normal distribution. The diagnostic ability of PET and MR were assessed through Receiver Operating Curve (ROC)-analysis for clustered data to account for the assessment of multiple segments per patient (Obuchowski, 1997). PET and MR measurements served as predictor variables in a binary logistic regression model to compute a prognostic score through the linear predictor of the model (linear predictor = -1.3487 - 0.6150 * FDG + 0.5909 * LGE). Hybrid imaging was compared to PET or MR results alone by use of this score. All statistical hypothesis testing has been performed on exploratory two-sided 5% significance levels. R 3.6.1 (The R Foundation for Statistical Computing, Vienna, Austria) has been used for computations.

5. Results

5.1 Baseline characteristics

Patient characteristics for the study group undergoing both imaging studies (n=23**)** are summarized in **Table 1.** Mean age in this cohort of patients affected by coronary artery disease (CAD) averaged 61±9 years. Leading cardiovascular risk factors were hypertension, followed by dyslipidaemia, a history of smoking, a positive CAD history in the family and about one fourth of the patients were diabetics. The majority (91%) of the patients showed a multivessel CAD and half (52%) of the patients had suffered from a previous myocardial infarction. Four patients had already undergone a bypass surgery. Most of the percutaneous interventions were undertaken in the RCA (56%), followed by LCx and LAD. In the coronary angiography most patients showed a right coronary dominancy (n=15, 65%) or a codominancy (n=6, 26%).

	Baseline Characteristics (n=23)
Male sex	22 (96%)
Age, years	61 ± 9
Body Mass Index, kg/m^2	29 ± 3
Diabetes	6 (26%)
Hypertension	21 (91%)
Smoking	13 (56%)
Dyslipidaemia	18 (78%)
Family history	6 (26%)
Multivessel CAD	21 (91%)
Previous myocardial infarction	12 (52%)
Coronary artery bypass	4 (17%)
Localization	LAD 4 (18%) LCX 6 (26%) RCA 13 (56%)
Coronary dominance	Right 15 (65%) Left 2 (9%) Codominant 6 (26%)

Table 1. Baseline characteristics of the patients' cohort. Data are expressed as mean ± standard deviation (SD) or as number of individuals and percentage of the total.

5.2 PET/MR imaging prior to revascularization

Combined PET/MR imaging was successfully performed in all 23 patients who underwent revascularization and follow-up imaging. In total n=391 segments were analyzed. Accounting for the individual anatomy showed by the coronary angiography, n=124 segments were assigned to the CTO-subtended territory.

FDG-PET viability

The vast majority of the entire LV segments analyzed by PET (n=383/391; 98.0%) were viable, as defined by an FDG uptake higher than the 50% of the reference area. In all segments assigned to the CTO territory, the prevalence of viability was comparably high (n=119/124, 96,0%). Those CTO-segments displaying a wall motion abnormality at baseline (n=80), viability was slightly lower (n= 75/80, 93.8%).

MR imaging

The presence of any LGE was detectable in every patient, affecting 28.6% of the overall segments cohort (n=112/391). However, about 90% of all segments (n =352/391) were defined viable, based on a transmural LGE extent <50%. The global size of LGE within the left ventricle at baseline averaged 9.9 ± 8.7 ml, resulting in 6.3 % of the LV. CTO-subtended segments displayed a higher proportion of LGE (n=68/124, 55%), and a significant drop in the proportion of MR viable segments (n= 96/124, 77%, p=0.0003) as compared to the entire cohort.

Regional contractility revealed an impaired wall motion in 168/391 (43.0%) segments in the overall cohort at baseline, whereas the CTO-subtended dysfuctional segments were 80/124 (64.5%). In those CTO-segments displaying a wall motion abnormality at baseline,

the presence of any LGE was 70% (56/80 segments) and the number of MR viable segments further declined (n =57/80, 71 %).

Mean global LV ejection fraction (EF) was slightly reduced at baseline (54.6%±14) but did not significantly change after successful revascularization (58.3% ±16, p=0.11). Also volumetric parameters as well as global LGE size did not change after revascularization between baseline and follow-up imaging (Table 2). After successful revascularization, 28% of the initially dysfunctional segments (22/80 segments) showed significant overall improvement in regional wall motion (p=0.014) (Figure 5).

n=23	Baseline	Follow-Up	p value
Tissue volume	133.6 ± 34.1 ml	140.2 ± 35.5 ml	0.14
EDV	150.2 ± 41.9 ml	146,6 ± 35.2 ml	0.57
ESV	68.9 ± 32.2 ml	63.5 ± 33.1 ml	0.22
EF	54.6 ± 13.8 %	58.3 ± 16.1 %	0.11
LGE Extent (ml)	9.9 ± 8.7 ml	9.7 ± 10.7 ml	0,97
LGE Extent (%LV)	6.3 ± 5.2 %	6.3 ± 5.5 %	0.95

Table 2. Global left ventricular parameters at baseline and follow-up. Data are expressed as mean ± SD.

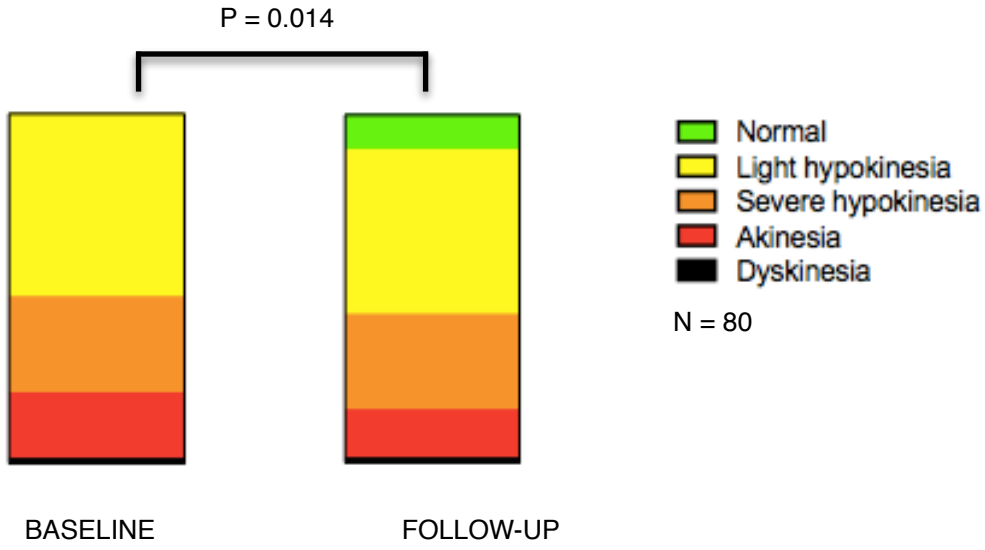

Figure 5. Significant improvement of wall motion abnormality score between baseline and follow up in the cohort of dysfunctional segments at baseline (n=80, p value =0.014).

5.3 Comparison between PET and MR imaging

Table 3 summarizes the PET and MRI viability results for the entire and CTO segments.

Both modalities demonstrated concordant viability results in 89.5% of all segments resulting in a slight intermethod agreement (k = .1).

The overall agreement between FDG uptake and LGE transmurality within CTO subtended dysfunctional segments dropped to 70%, (k = .04). In these segments, PET/MR concordantly identified n=54 viable (68%) and n=2 non-viable segments (2%). However, 30% of these segments showed a discordant viability pattern by both methods. PET viable, but MR non-viable results were detected within n=21 segments (26%), and PET non-viable, but MR viable in n=3 segments (4%).

Regional wall motion differed among the different PET/MR subgroups **(Table 4)**. PET viable/ MR non-viable segments revealed a significantly more impaired wall motion abnormality score at baseline than segments with concordant evidence of viability by PET and MRI (p=0.019).

While improvement of regional wall motion abnormality score between baseline and follow up was not significant within those segments displaying a concordant viability by both PET and MRI **(Figure 6A)**, segments with a discordant pattern of viability (PET viable/ MR non-viable) demonstrated a significant improvement of regional contractility (p-value = 0.033) **(Figure 6B)**.

All segments n=391	PET viable	PET non viable	
MR viable	347 (89%)	5 (1%)	352 (90%)
MR non viable	36 (9%)	3 (1%)	39 (10%)
	383 (98%)	8 (2%)	

CTO-subtended segments n=124	PET viable	PET non viable	
MR viable	93 (75%)	3 (2%)	96 (77%)
MR non viable	26 (21%)	2 (2%)	28 (23%)
	119 (96%)	5 (4%)	

CTO-subtended Segments with WMA n=80	PET viable	PET non viable	
MR viable	54 (67%)	3 (4%)	57 (71%)
MR non viable	21 (26%)	2 (3%)	23 (29%)
	75 (93%)	5 (7%)	

Table 3. Distribution of the whole cohort of LV segments (above), of the subcohort of CTO-subtended segments (middle) and the subcohort of CTO-subtended dysfunctional segments (below) by the viability pattern in PET-MR.

	CTO-subtended segments with WMA n=80	Median abnormality score baseline		Median abnormality score follow up	p value
PET viable MR viable	54 (67,5%)	1	P = 0.019	1	0.21
PET viable MR non-viable	21 (26,25%)	2		1	0.03

Table 4. Summary of wall motion abnormality scores at baseline and follow-up of the PET viable/MR non-viable subgroup and the PET viable/ MR non-viable subgroup.

Figure 6A and 6B. Wall motion abnormality score at baseline and follow up in the PET viable/MRI viable subgroup (A) and in the PET viable/MRI non viable subgroup (B).

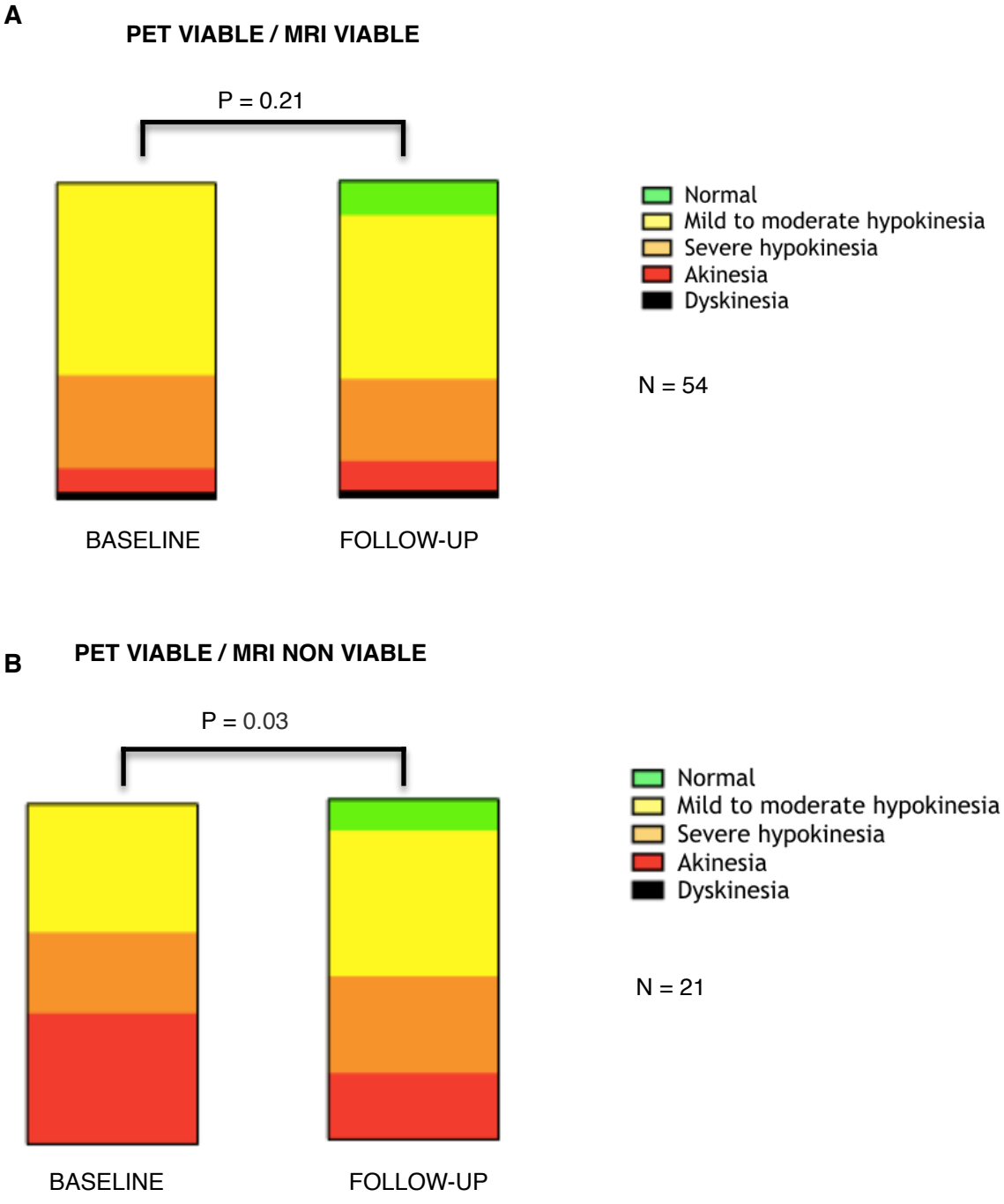

5.4 Diagnostic value of combined PET/MR imaging

Based on the ROC analysis for the prediction of wall motion recovery of the myocardial segments after CTO revascularization, the areas under the curve (AUC) for both imaging modalities alone were 0.58 (SE: 0.10) for FDG-PET, and 0.66 (SE: 0.09) for LGE MR, respectively (Figure 7). The combined information of PET and MR imaging together resulted in a clear improvement of the diagnostic accuracy expressed by the increase of the AUC achieving 0.72 (SE: 0.07) with an associated p-value p= 0.002, which was 6% superior than LGE in MR and 13% superior than FDG PET (AUC=0.58, SE= 0.10) alone (Figure 8).

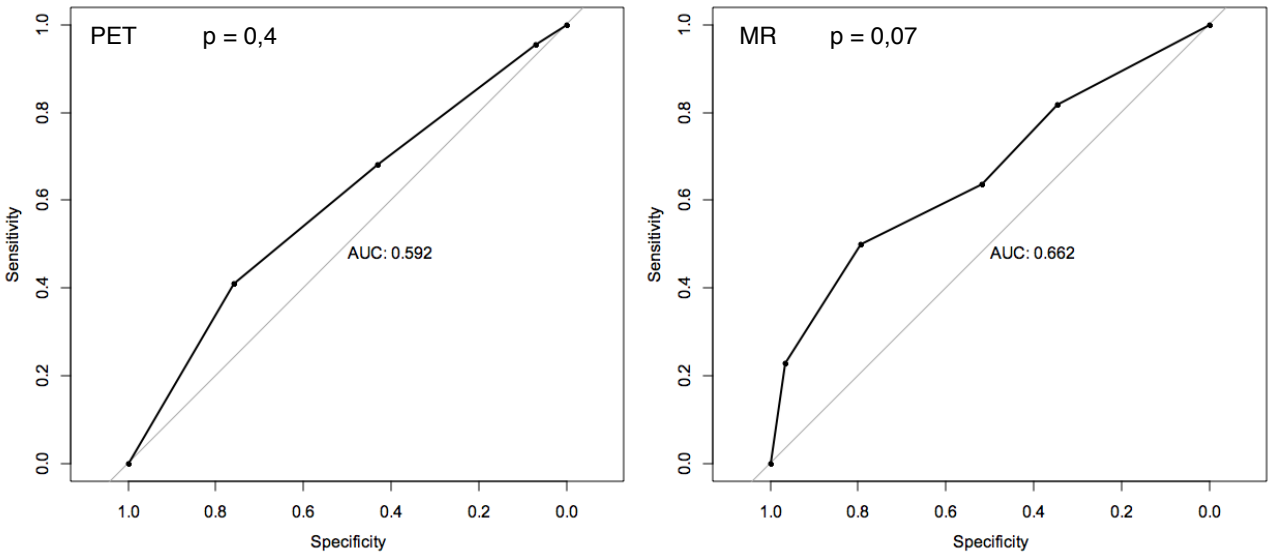

Figure 7. ROC curves for FGD PET (left) and MRI (right).

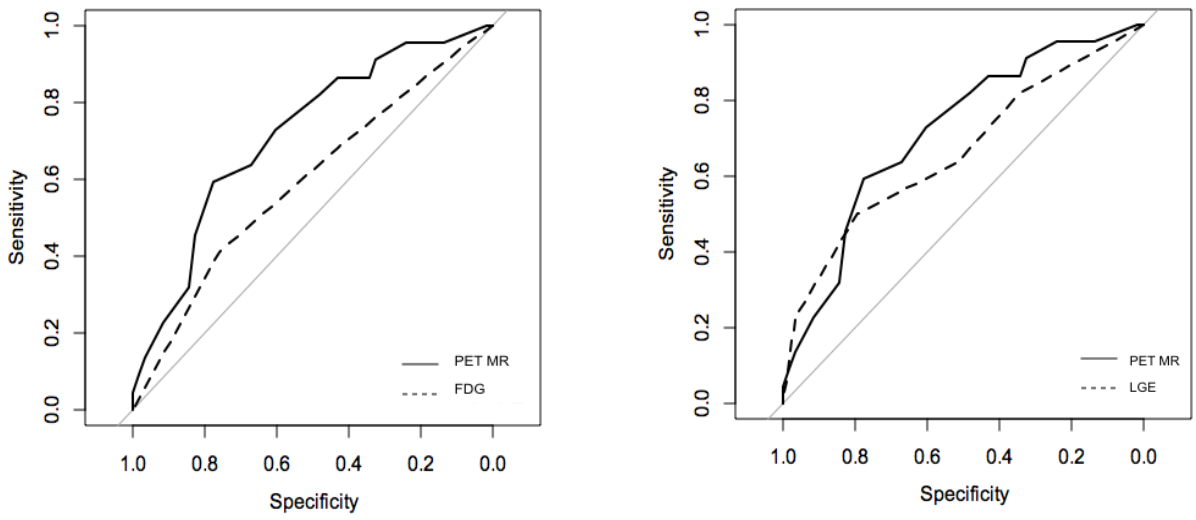

Figure 8. Comparison of the ROC curve obtained from the PET/MR score with PET-FDG (left) and LGE (right) respectively. The AUC (SE) for the PET/MR ROC curve was 0.72 (0.07), for PET-FDG 0.58 (0.10) and for LGE 0.66 (0.09).

6. Discussion

The major finding of this study is that simultaneous hybrid PET/MR imaging predicts more accurately regional wall motion recovery after CTO revascularization, in comparison to PET or MR alone. Combined imaging allowed the detection of dysfunctional segments with high ischemic burden (PET viable/ MRI non-viable) still presenting recovery potential, which may benefit from revascularization.

Revascularization of CTO has been associated with recovery of impaired left ventricular function and improved survival (Galassi et al. 2015, Stuijfzand et al., 2017). In presence of wall motion abnormalities, viability imaging is recommended prior to CTO revascularization by the 2018 ESC/EACTS guidelines in order to determine the amount of viable myocardium and thus the likelihood to anticipate improvement of contractility. However, registration of transmural myocardial viability based on dichotomous criteria may be challenging particularly within myocardium, since it may encompass various tissue conditions side by side, including perfused or ischemic hibernation with or without myocardial shrinkage.

6.1 Comparison of PET vs. MRI for viability assessment

Several non-invasive imaging modalities have been introduced for the identification and assessment of myocardial viability, whereby FDG-PET is currently regarded as the clinical gold standard (Stuijfzand WJ et al., 2015). Observational evidence suggests that FDG-PET has the greatest sensitivity in predicting global LV functional recovery following revascularization, compared with other imaging modalities (Rischpler et al., 2015). On the other hand, techniques such as cardiac MRI and stress-echocardiography may show a higher specificity (Santos et al., 2019).

In literature, regional FDG uptake in PET of more than 50% compared with remote myocardium and a LGE transmurality in MRI of less than 50% of the ventricular wall are generally accepted markers defining viable myocardium, which have shown to have the potential to improve after revascularization (Rischpler et al, 2015). Based on these thresholds, we obtained only a slight intermethod agreement for FDG-PET and LGE-MRI in our cohort. While 94% of the ischemic dysfunctional CTO-segments with wall motion abnormality were PET viable, MR identified only 71% of these segments as viable. This discrepancy may at least partly be explained by the intrinsically higher spatial resolution of MR imaging compared to PET, allowing the detection of even small sections of transmural scar enhancement with higher sensitivity as compared to nuclear techniques, which could lead to classification as avital in segments with borderline findings (i.e. approximately 50% transmurality) (Ibrahim et al. 2009). Another fundamental difference between the two methods is that LGE MRI displays extracellular matrix expansion (i.e. avital tissue/edema), while FDG PET maps the vital, glucose-consuming myocytes. Moreover, due to the non-specificity – from the physiological perspective - of gadolinium-based MR contrast media, the focal increase in myocardial extracellular volume as indicated by LGE can in fact be observed in various clinical pathologies including fibrosis, inflammation, edema and cardiac storage disorders (Captur et al, 2016). Therefore, LGE alone may present limited power in the differentiation between these tissue states which can be increased by expansion of the MRI acquisition protocol for instance by T2-weighted imaging or perfusion sequences (Captur et al., 2016). Since we did not perform MR-perfusion imaging, we were not able to reliably identify hibernating myocardium, i.e. hypoperfused, dysfunctional myocardium that is still viable and shows a very high likelihood of recovery after revascularization. Adding perfusion to the viability study would very likely increase specificity in the identification of segments with high likelihood of recovery after revascularization, as only this approach al-

lows to distinguish between viable and hibernating vs. viable but not hibernating myocardium (Bucciarelli-Ducci et al., 2016). Wang et al. already correlated hibernating myocardium in perfusion/metabolism PET imaging with LGE extent in patients with CTO. The study showed that not only segments with non-transmural LGE had great probability of having hibernating tissue, but also one-third of segments with transmural scar in MRI still showed myocardial hibernation (Wang et al., 2018).

On the contrary, FDG-PET definitely adds sensitivity in identifying small amounts of still viable epicardial myocardium even in the presence of large myocardial scars (LGE>50% of myocardial thickness). The subepicardial FDG activity is able to show different properties of myocardium including hibernation, stunning and normal myocardium (Wang et al, 2017).

In our cohort we found a large prevalence, about one quarter of CTO-segments (26%), with a discordant viability pattern, mostly showing viability in PET and non-viability in MRI. This combination allowed to identify those segments displaying a high regional wall motion abnormality and high potential for recovery of function after CTO revascularization. In fact, it was the only combination (PET viable/ MRI non-viable) in our cohort to show a significant improvement of wall motion abnormality at follow-up. Hence, this particular pattern of viability may allow the identification of highly ischemic and dysfunctional myocardium, which could benefit substantially from revascularization. The prevalence of this combination (PET viable/ MRI non-viable) was relatively high in our patient population suffering from chronic-ischemic, mostly multivessel coronary artery disease. Conversely, in a recent study in patients with acute myocardial infarction and successful reperfusion, in which myocardial stunning may have primarily dominated, this discordant viability pattern (PET viable/ MRI non-viable) was not commonly described (Rischpler et al. 2015).

6.2 Diagnostic value of combined PET/MR

This is the first study that sought to assess regional myocardial viability by simultaneous PET/MR imaging in patients undergoing a CTO revascularization. Using a hybrid PET/MR scanner with integration of both modalities allowing a truly synchronous/simultaneous acquisition of complementary information such as high resolution anatomy and myocardial metabolism in merged images (Rischpler et al., 2013). Thus, the principle to combine different imaging modalities in order to increase the diagnostic accuracy in predicting myocardial viability and long-term improvement of regional impaired function is highly attractive. Based on the ROC-analysis, simultaneous PET/MR imaging was superior to LGE-MR or FDG-PET alone in predicting functional recovery after revascularization of CTO. Therefore, LGE-MR adds specificity to the investigation, outlining the segments with high burden of ischemia and wall motion dysfunction that could potentially benefit from revascularization.

The superiority in combining the complementary information from PET and MR has been demonstrated already in other clinical settings, such as in the diagnosis of cardiac sarcoidosis (Vita et al., 2018) or prostate cancer (Eiber et al, 2016), enhancing the value of hybrid PET/MR imaging in different fields.

Although we demonstrated a higher diagnostic accuracy in detecting regional functional improvement by simultaneous imaging of PET-FDG and MRI-LGE as compared to these modalities alone, we did not observe significant effects on global LV parameters. An explanation for this may be that the ejection fraction was only slightly impaired before revascularization of the CTO and that the global extent of LGE across the left ventricle was only 6.3±5.2%. Similarly, recent small- to moderate-sized cardiac MR imaging studies which evaluated CTO showed conflicting results or only minor improvements of LVEF (Pujadas et al, 2013; Chadid et al., 2015). Larger studies are warranted to further assess whether

revascularization of CTO based on hybrid imaging may have an impact on more established clinical outcome measures such as LV function or even mortality and thus provide evidence to become a meaningful approach in planning such interventions.

6.3 Limitations

This was a pilot study with a comprehensive protocol and therefore a relatively small number of patients were included, despite the involvement of three centres. Larger multicenter studies are warranted to confirm these preliminary results. The study population finally underwent hybrid PET/MRI, successful CTO-revascularization, as well as follow-up imaging, respectively. Moreover, the global LV function at baseline in this cohort was almost normal and thus the total amount of dysfunctional segments assigned to the CTO-territory were moderate. Only patients with successful CTO-revascularization underwent follow-up imaging, so we cannot comment on potential positive outcome measures on LV remodeling associated with CTO revascularization in comparison to patients after attempted PCI. In addition, this study did not assess the vessel patency at follow-up imaging. This may have led to an underestimation of LVEF and wall motion recovery, given a risk of re-occlusion after revascularization. In fact, Pujadas et al. observed an increase in EDV at 6 months follow-up after a failed procedure, suggesting the progression of negative LV remodelling over time in the presence of a persisting CTO. Moreover, recovery of dysfunctional myocardium after revascularization is affected by a number of factors such as prolonged duration of the coronary occlusion, severe LV remodeling, re-occlusion, procedure related necrosis and does not necessarily imply an failure in the viability assessment (Shah et al., 2013).

Finally, in order to facilitate straightforward imaging, a MR protocol without sequences such as perfusion imaging were applied, which could have improved the detection of myocardial hibernation.

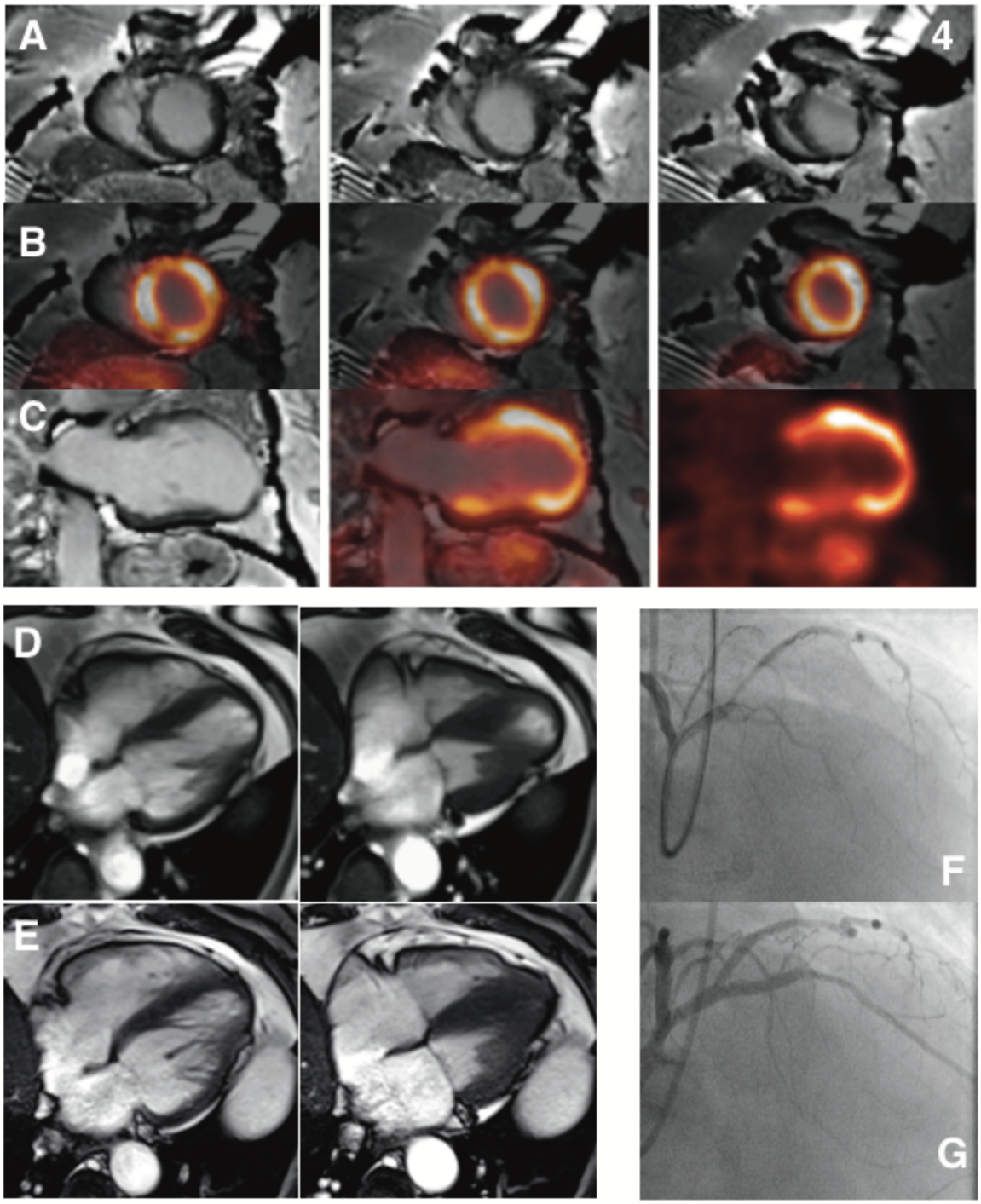

Figure 9. Example of a patient with a CTO of the LAD. In A, MRI short axis slices show a thinned anteroseptal left ventricular wall with non-transmural LGE. PET/MR fused short axis acquisition are presented in B, showing an overall PET-viable myocardium. C shows a 2-chamber view of fused PET/MR acquisition. Enddiastolic (left) and endsystolic (right) cine sequences in 4-chamber view at baseline (D) and at follow-up (E) show an improvement of the hypokinesia of the apex. Coronary angiography of the CTO of the LAD before (F) and after successful revascularization (G).

7. Conclusions

Hybrid PET/MR imaging prior to successful CTO revascularization showed a better performance than PET or MRI alone in predicting regional improvement of disturbed wall motion in territories affected by CTO. The complimentary information derived from both modalities may particularly help to identify small amounts of viable, dysfunctional and hibernating epicardial myocardium within large scars, which have the potential to improve contractility after CTO-revascularization.

8. Acknowledgements

We gratefully acknowledge PD Dr. Alexander Hapfelmeier for the assistance in the statistical analysis and the excellent technical assistance of Sylvia Schachoff.

9. References

Allmann KC, Noninvasive assessment myocardial viability: Current status and future directions J Nucl Cardiol 2013;29:618-37

Anagnostopoulos C, Georgakopoulos A, Pianou N, Nekolla SG: Assessment of myocardial perfusion and viability by positron emission tomography. Int J Cardiol 2013;167:1737-49.

Baer FM, Voth E, Deutsch HJ, Schneider CA, Horst M, de Vivie ER et al. Predictive value of low dose dobutamine transesophageal echocardiography and fluorine-18 fluorodeoxyglucose positron emission tomography for recovery of regional left ventricular function after successful revascularization. J Am Coll Cardiol 1996;28:60–9.

Bucciarelli-Ducci C, Auger D, Di Mario C, Locca D, Joanna Petryka J, Hanlon RO, Grasso A, Christine Wright C, Symmonds K, Wage R, Eleni Asimacopoulos E, Del Furia F, Lyne JC, GatehousePD, Fox KM, Pennell DJ CMR Guidance for Recanalization of Coronary Chronic Total Occlusion ACC Cardiovasc Imaging. 2016;9(5):547-56.

Captur G, Manisty C, Moon JC Cardiac MRI evaluation of myocardial disease Heart 2016;102:1429-1435.

Cassen B, Theory of the performance characteristics of radioisotope distribution imaging systems. J Nucl Med. 1964 Feb;5:95-10

Cerqueira MD, Weissman NJ, Dilsizian V, Jacobs AK, Kaul S, Laskey WK et al. Standardized myocardial segmentation and nomenclature for tomographic imaging of

the heart. A statement for healthcare professionals from the Cardiac Imaging Committee of the Council on Clinical Cardiology of the American Heart Association. Circulation 2002;105:539–42

Chadid P, Markovic S, Bernhardt P, Hombach V, Rottbauer W, Wöhrle J. Improvement of regional and global left ventricular function in magnetic resonance imaging after recanalization of true coronary chronic total occlusions. Cardiovasc Revasc Med. 2015;16:228-32.

DeFronzo RA, Tobin JD, Andres R. Glucose clamp technique: a method for quantifying insulin secretion and resistance. Am J Physiol 1979;237:E214–23.

Delso G, Furst S, Jakoby B, Ladebeck R, Ganter C, Nekolla SG et al. Performance measurements of the Siemens mMR integrated whole-body PET/MR Scanner. J Nucl Med 2011;52:1914–22

Dilsizian V, Bacharach SL, Beanlands RS, Bergmann SR, Delbeke D, Gropler RJ, Knuuti J, Schelbert HR, Travin MI: ASNC imaging guidelines for nuclear cardiology procedures. PET myocardial perfusion and metabolism clinical imaging. J Nucl Cardiol 2009;651–651

Drzezga A, Souvatzoglou M, Eiber M, Beer AJ, Fürst S, Martinez-Möller A, Nekolla SG, Ziegler S, Ganter C, Rummeny EJ, Schwaiger M. First clinical experience with integrated whole-body PET/MR: comparison to PET/CT in patients with oncologic diagnoses. J Nucl Med. 2012;53(6):845-55.

Eiber M, Weirich G, Holzapfel K, Souvatzoglou M, Haller B, Rauscher I, Beer AJ, Wester HJ, Gschwend J, Schwaiger M, Maurer T Simultaneous 68Ga-PSMA HBED-CC PET/MRI Improves the Localization of Primary Prostate Cancer Eur Urol. 2016;70(5):829-836.

Galassi AR, Sianos G, Werner GS, Escaped J, Tomasello SD, Boukhris M, Castaing M, Büttner JH, Bufe A, Kalnins A, Spratt JC, Garbo R, Hildick-Smith D, Elhadad S, Gagnor A, Lauer B, Bryniarski L, Christiansen EH, Thuesen L, Meyer-Geßner M, Goktekin O, Carlino M, Louvard Y, Lefevre T, Lismanis A, Galev VI, Serra A, Marza´ F, Di Mario C, Reifart N. Retrograde Recanalization of Chronic Total Occlusions in Europe, J Am Coll Cardiol 2015;65:2388–400

Gambhir SS, Schwaiger M, Huang SC, Krivokapich J, Schelbert HR, Nienaber CA, Phelps ME. Simple noninvasive quantification method for measuring myocardial glucose utilization in humans employing positron emission tomography and fluorine-18 deoxyglucose J Nucl Med. 1989;30(3):359-66.

Hoebers LP, Claessen BE, Dangas GE, Råmunddal T, Mehran R Henriques JPS. Contemporary overview and clinical perspectives of chronic total occlusions Nat. Rev. Cardiol, 2014;11:458–469

Ibrahim T, Hackl T, Nekolla SG, Breuer M, Feldmair M, Schömig A, Schwaiger M Acute myocardial infarction: serial cardiac MR imaging shows a decrease in delayed enhancement of the myocardium during the 1st week after reperfusion Radiology. 2010 Jan;254(1): 88-97

Kaandorp TAM, Lamb HJ, van derWall EE, de Roos A, Bax JJ Cardiovascular MR to assess myocardial viability in chronic ischemic LV Dysfunction Heart 2005;91:1359–1365

Kirschbaum SW, Rossi A, Boersma E, Springeling T, van de Ent M, Krestin GP, Serruys PW, Duncker DJ, de Feyter PJ, van Geuns R-J M. Combining magnetic resonance viability variables better predicts improvement of myocardial function prior to percutaneous coronary intervention Int J Cardiol 2012;159:192–197.

Klein C, Nekolla SG, Bengel FM, Momose M, Sammer A, Haas F, Schnackenburg B, Delius W, Mudra H, Wolfram D, Schwaiger M. Assessment of myocardial viability with contrast-enhanced magnetic resonance imaging: comparison with positron emission tomography. Circulation. 2002;105(2):162-7.

Koelbl CO, Nedeljkovic ZS, Jacobs AK. Coronary Chronic Total Occlusion (CTO): A Review Rev. Cardiovasc. Med. 2018;19(1): 33–39.

Krumm, P, Mangold S, Gatidis S, Nikolaou K, Nensa F, Bamberg F, La Fougère C Clinical use of cardiac PET/MRI: current state-of-the-art and potential future applications. Jpn J Radiol 2018;36(5):313–323.

Kwong RY, Chan AK, Brown KA, Chan CW, Reynolds HG, Tsang S et al. Impact of unrecognized myocardial scar detected by cardiac magnetic resonance imaging on event-free survival in patients presenting with signs or symptoms of coronary artery disease. Circulation 2006;113:2733–43.

Levine GN, Bates ER, Blankenship JC 2011 ACCF/AHA/SCAI Guideline for percutaneous coronary intervention. J Am Coll Cardiol 2011;58, e44-122

Löffler AI, Kramer CM Myocardial Viability Testing to Guide Coronary Revascularization Intervent Cardiol Clin, 2018;7,355–365

Martinez-Moller A, Souvatzoglou M, Delso G, Bundschuh RA, Chefd'hotel C, Ziegler SI et al. Tissue classification as a potential approach for attenuation correction in whole-body PET/MRI: evaluation with PET/CT data. J Nucl Med 2009;50:520–6.

Nekolla SG, Miethaner C, Nguyen N, Ziegler SI, Schwaiger M. Reproducibility of polar map generation and assessment of defect severity and extent assessment in myocardial perfusion imaging using positron emission tomography. Eur J Nucl Med 1998;25:1313–21.

Neumann FJ, Sousa-Uva M, Ahlsson A, Alfonso F, Banning AP, Benedetto U, Byrne RA, Collet JP, Falk V, Head SJ, Jüni P, Kastrati A, Koller A, Kristensen SD, Niebauer J, Richter DJ, Seferović PM, Sibbing D, Stefanini GG, Windecker S, Yadav R, Zembala MO, 2018 ESC/EACTS Guidelines on myocardial revascularization, European Heart Journal 2019;40:87–165

Nuyts J, Bal G, Kehren F, Fenchel M, Michel C,Watson C. Completion of a truncated attenuation image from the attenuated PET emission data. IEEE Trans Med Imaging 2013;32:237–46.

Obuchowski, NA, Nonparametric analysis of clustered ROC curve data. Biometrics 1997:567-578.

Pinak B.S. Management of coronary total occlusion. Circulation 2011;123:1780-1784.

Pujadas S, Martin V, Rosselló X, Carreras F, Barros A, Leta R, Alomar X, Cinca J, Sabate M, Pons-Llado G, Improvement of myocardial function and perfusion after successful percutaneous revascularization in patients with chronic total coronary occlusion Int J Cardiol 2013;169:147–152

Rischpler C, Langwieser N, Souvatzoglou M, Batrice A, van Marwick S, Snajberk J, Ibrahim T, Laugwitz KL, Nekolla SG, Schwaiger M PET/MRI early after myocardial infarction: evaluation of viability with late gadolinium enhancement transmurality vs. ^{18}[F]-FDG uptake Eur Heart J 2015;16:661-669

Rischpler C, Nekolla SG, Dregely I, Schwaiger M. Hybrid PET/MR imaging of the heart: potential, initial experiences, and future prospects. J Nucl Med 2013;54(3):402-15.

Sachdeva R, Agrawal M, Flynn SE, Werner GS, Uretsky BF. The myocardium supplied by a chronic total occlusion is a persistently ischemic zone. Catheter Cardiovasc Interv. 2014;83:9-16.

Santarelli MF: Physical principles of imaging with magnetic resonance. In: MRI of the heart and vessels. Lombardi M and Bartolozzi C eds Springer-Verlag Publ, Milan, Italy, 2005 pp 1-30.

Santos BS, Ferreira MJ. Positron emission tomography in ischemic heart disease. Rev Port Cardiol. 2019;38(8):599-608.

Sarikaya, I. Cardiac applications of PET. Nuclear Medicine Communications, 2015;36(10): 971–985.

Schindler TH, Schelbert HR, Quercioli A, Dilsizian V: Cardiac PET Imaging for the detection and monitoring of coronary artery disease and microvascular health. J Am Coll Cardiol Img 2010;3:623-640.

Schinkel AF, Bax JJ, Poldermans D, Elhendy A, Ferrari R, Rahimtoola SH. Hibernating myocardium: diagnosis and patient outcomes. Curr Probl Cardiol 2007;32:375–410.

Schwaiger M, Brunken RC, Krivokapich J, Child JS, Tillisch JH, Phelps ME, Schelbert HR. Beneficial effect of residual anterograde flow on tissue viability as assessed by positron emission tomography in patients with myocardial infarction. Eur Heart J. 1987;8(9):981-8.

Shah BN, Khattar RS, Senior R. The hibernating myocardium: current concepts, diagnostic dilemmas, and clinical challenges in the post-STICH era Eur Heart J 2013;34:1323–1334.

Stuijfzand WJ, Biesbroek PS, Raijmakers PG, Driessen RS, Schumacher SP, van Diemen, van den Berg J, Nijveldt R, Lammertsma AA, Walsh SJ, Hanratty CG, Spratt JC, van Rossum AC, Nap A, van Royen N, Knaapen P. Effects of successful percutaneous coronary intervention of chronic total occlusions on myocardial perfusion and left ventricular function EuroIntervention 2017;13:345-354

Stuijfzand WJ, Driessen RS, Raijmakers PG, Rijnierse MT, Maeremans J, Hollander MR, Lammertsma AA, van Rossum AC, Dens J, Nap A, van Royen N, Knaapen P Prevalence

of ischemia in patients with a chronic total occlusion and preserved left ventricular ejection fraction Eur Heart J Cardiovasc Imaging. 2017;18(9):1025-1033

Stuijfzand WJ, Raijmakers PG, Driessen RS, Nap A, van Rossum AC, Knaapen P. Value of Hybrid Imaging with PET/CT to Guide Percutaneous Revascularization of Chronic Total Coronary Occlusion Curr Cardiovasc Imaging Rep. 2015;8(7):26.

Suero JA, Marso SP, Jones PG, Laster SB; Huber KC, Giorgi LV, Johnson WL, Rutherford BD Procedural outcomes and long-term survival among patients undergoing percutaneous coronary intervention of a chronic total occlusion in native coronary arteries: a 20-year experience J Am Coll Cardiol 2001;38(2):409-414

Timmis A, Townsend N, Gale C, Rick Grobbee, Nikos Maniadakis, Marcus Flather, Elizabeth Wilkins, Lucy Wright, Rimke Vos, Jeroen Bax, Maxim Blum, Fausto Pinto, Panos Vardas, ESC Scientific Document Group, European Society of Cardiology: Cardiovascular Disease Statistics 2017, European Heart Journal 2018;39(7): 508–579

Torigian DA, Zaidi H, Kwee TC, Saboury B, Udupa JK, Cho ZH et al. PET/MR imaging: technical aspects and potential clinical applications. Radiology 2013;267:26–44.

Vita T, Okada DR, Veillet-Chowdhury M, Bravo PE, Mullins E, Hulten E, Agrawal M, Madan R, Taqueti VR, Steigner M, Skali H, Kwong RY, Stewart GC, Dorbala S, Di Carli MF, Blankstein R Complementary Value of Cardiac Magnetic Resonance Imaging and Positron Emission Tomography/Computed Tomography in the Assessment of Cardiac Sarcoidosis. Circ Cardiovasc Imaging. 2018;11:e007030.

Wang L, Lu M, Feng L, Wang J, Fang W, He Z, Dou K, Zhao S, Yang M. Relationship of myocardial hibernation, scar, and angiographic collateral flow in ischemic cardiomyopathy with coronary chronic total occlusion J Nucl Cardiol 2019;26:1720-1730

Werner GS, Martin-Yuste V, Hildick-Smith D, Boudou N, Sianos G, Gelev V, Rumoroso JR, Erglis A, Christiansen EH, Escaned J, di Mario C, Hovasse T, Teruel L, Bufe A, Lauer B, Bogaerts K, Goicolea J, Spratt JC, Gershlick AH, Galassi AR, Louvard Y. EUROCTO trial investigators. A randomized multicentre trial to compare revascularization with optimal medical therapy for the treatment of chronic total coronary occlusions. Eur Heart J 2018;39(26):2484-2493